


RESEARCH ARTICLE

Optimized microburst VNS elicits fMRI responses beyond thalamic-specific response from standard VNS

Jerzy P. Szaflarski¹ , Jane B. Allendorfer¹, Jason Begnaud², Giovanni Ranuzzi², Elhum Shamshiri², Ryan Verner² & for the Microburst Study Group*

¹Department of Neurology and the UAB Epilepsy Center, Heersink School of Medicine, University of Alabama at Birmingham, Birmingham, Alabama, USA

²LivaNova Inc, Houston, Texas, USA

Correspondence

Jerzy P. Szaflarski and Jane B. Allendorfer, UAB Epilepsy Center, 312 Civitan International Research Center, 1719 6th Avenue South, Birmingham, AL, USA. Tel: 205.975.5587; E-mail: jszaflarski@uabmc.edu; jallendorfer@uabmc.edu

Funding Information

This study was supported by LivaNova Inc. Dr. Szaflarski and Dr. Allendorfer received continuous consulting support for study development, implementation, and for data analysis pipeline development and implementation. Final data analyses and reporting were supported by a separate grant from LivaNova Inc. to JPS. Drs. Begnaud, Ranuzzi, Shamshiri, and Verner are employees of LivaNova Inc.

Received: 24 August 2023; Revised: 21 December 2023; Accepted: 14 February 2024

Annals of Clinical and Translational Neurology 2024; 11(5): 1135–1147

doi: 10.1002/acn3.52029

*Microburst study group is listed in the Acknowledgments.

Abstract

Objective: In parallel to standard vagus nerve stimulation (VNS), microburst stimulation delivery has been developed. We evaluated the fMRI-related signal changes associated with standard and optimized microburst stimulation in a proof-of-concept study (NCT03446664). **Methods:** Twenty-nine drug-resistant epilepsy patients were prospectively implanted with VNS. Three 3T fMRI scans were collected 2 weeks postimplantation. The maximum tolerated VNS intensity was determined prior to each scan starting at 0.125 mA with 0.125 mA increments. fMRI scans were block-design with alternating 30 sec stimulation [ON] and 30 sec no stimulation [OFF]: Scan 1 utilized standard VNS and Scan 3 optimized microburst parameters to determine target settings. Semi-automated on-site fMRI data processing utilized ON–OFF block modeling to determine VNS-related fMRI activation per stimulation setting. Anatomical thalamic mask was used to derive highest mean thalamic *t*-value for determination of microburst stimulation parameters. Paired *t*-tests corrected at $P < 0.05$ examined differences in fMRI responses to each stimulation type. **Results:** Standard and microburst stimulation intensities at Scans 1 and 3 were similar ($P = 0.16$). Thalamic fMRI responses were obtained in 28 participants (19 with focal; 9 with generalized seizures). Group activation maps showed standard VNS elicited thalamic activation while optimized microburst VNS showed widespread activation patterns including thalamus. Comparison of stimulation types revealed significantly greater cerebellar, midbrain, and parietal fMRI signal changes in microburst compared to standard VNS. These differences were not associated with seizure responses. **Interpretation:** While standard and optimized microburst VNS elicited thalamic activation, microburst also engaged other brain regions. Relationship between these fMRI activation patterns and clinical response warrants further investigation. Clinical Trial Registration: The study was registered with clinicaltrials.gov (NCT03446664).

Introduction

Open-loop vagus nerve stimulation (VNS) therapy has been a staple for the management of patients with difficult to control focal-onset seizures with the approval age starting as early as 4 years. This therapy is also frequently used for the treatment of patients with generalized and other seizure types.¹ The stimulation parameters and

adjustment methods have remained relatively unchanged over time.² The efficacy of VNS for the treatment of drug-resistant seizures was proven in four randomized controlled trials with pooled mean percentage decrease in seizure frequency at the last follow-up of 34% and pooled probability of being a responder ($\geq 50\%$ seizure reduction) of 42.7%.^{1,3} While these numbers indicate reasonable efficacy, one may ask if there is a possibility of adjusting or

changing the stimulation parameters in order to provide better seizure control while also decreasing the potential for adverse events related to VNS.

The fields of neurostimulation and neuromodulation have undergone substantial development.⁴ Depending on the characteristics of the delivered stimuli, direct or indirect neurostimulation and neuromodulation can excite or inhibit neurons via GABA-ergic and NMDA-mediated mechanisms.^{4,5} One of the important recent developments was implementation of a novel noninvasive stimulation paradigm called intermittent theta burst stimulation (iTBS).⁶ This protocol provides a stimulation approach that, depending on the parameters used and stimulation site employed, affects long-term potentiation or inhibition with a single course stimulation delivery altering the network responses for up to 1 h and resulting in short- and intermediate network plasticity.^{6,7} A stimulation protocol that includes iTBS is known to mimic the electrical firing of the hippocampus, and such protocol may have some theoretical advantages in the long-term treatment studies over continuous or prolonged and sustained stimulation.⁸ Microburst VNS uses high frequency bursts of VNS in a manner similar to iTBS, is similarly biomimetic in its mimicry of the calcium bursts, and has been shown to modulate interactions between the vagus nerve and the thalamic nuclei.⁹ The microburst protocol previously tested in primates is the basis of the microburst protocol implemented in the present study (Fig. 1A).

Several direct studies have investigated the effects of VNS therapy on the brain. The abovementioned primate study recorded evoked potentials in the thalamus in response to the stimulation of the vagus nerve.⁹ The specific thalamic nuclei that showed responses included not only the intralaminar but also the adjacent parafascicular nuclei. A follow-up primate study tested afferent anatomical connectivity of the parafascicular nucleus to show structural connections to caudate, putamen, and striatum.¹⁰ These findings were recently expanded via rodent studies. In one study, VNS stimulation resulted in cellular and metabolic changes in thalamus and other regions in stimulated rodents.¹¹ In another study, stimulation of locus coeruleus (an important nucleus associated with vagus nerve) via burst paradigms improved neuronal synchronization, a finding that was not replicated with standard VNS paradigm.¹² While the standard VNS paradigm elicited the most consistent locus coeruleus response, a microburst paradigm with seven pulses per second separated by 1 sec between bursts was best for eliciting increased response.¹² Another study implicated the afferent connections of the nucleus tractus solitarius in the VNS response.¹³ In a different study, VNS increased immediate and 1-week seizure threshold in a kindling model of epilepsy in rodents when using standard and

microburst stimulation parameters.¹⁴ However, the effect was observed at lower stimulation levels in animals that received the microburst protocol vs. the animals that received standard stimulation (0.25 vs. 0.5 mA, respectively). These studies clearly implicate thalamus and its afferent projections in seizure generation and maintenance and suggest that modulating these connections may affect seizure occurrence.

Human translation of animal studies is of paramount importance. While it is not possible to use direct electrode implants solely for human experimentation, human neuroimaging studies may provide indirect evidence for the involvement of these structures in the VNS mechanism of action (MOA). A comparison of low- and high-level standard stimulation parameters in 10 patients with epilepsy visualized, using H₂¹⁵O-PET, higher volume of activated tissue in the high-level stimulation group in multiple cortical and subcortical regions including bilateral thalami.¹⁵ A longitudinal follow-up study suggested that only thalamic regional cerebral blood flow changes mediated the antiseizure effects of VNS.¹⁶ Several functional MRI (fMRI) epilepsy studies were also conducted. While variable activation patterns were observed between studies, few of them warrant detailed discussion. In one study, different VNS pulse width was associated with different blood oxygenation level dependent (BOLD) responses indicating that lower pulse width (130 μs) may be insufficient to activate certain brain regions when compared to higher pulse width stimulation (250 or 500 μs); however, thalamic activations were not observed.¹⁷ In another study, thalamic (BOLD) signal increase was only seen in patients who exhibited improved seizure control while all patients had BOLD signal changes in frontal and occipital cortices.¹⁸ Finally, one study detected VNS-induced activation in multiple brain regions with the maximum BOLD signal changes observed in thalami and insulae.¹⁹ These studies show varying neuroimaging responses to VNS likely because of methods and cohorts used, small number of participants enrolled (highest $N = 11$ ¹⁶), and variable stimulation parameters. Yet, these studies confirmed several themes—the thalamus is frequently involved in response to VNS, the thalamic response may be associated with seizure response, the brain response may vary with stimulation parameters used, and various midline structures (based on animal studies) are involved in response to VNS therapy. However, it remains unclear whether the relationship between response to VNS and thalamic modulation is binary or proportional, that is, whether the degree of thalamic signal response is directly related to the degree of clinical treatment effect.

The goals of the present study were twofold—to firmly establish the typical brain response patterns to VNS using a large cohort of patients with focal- and generalized-

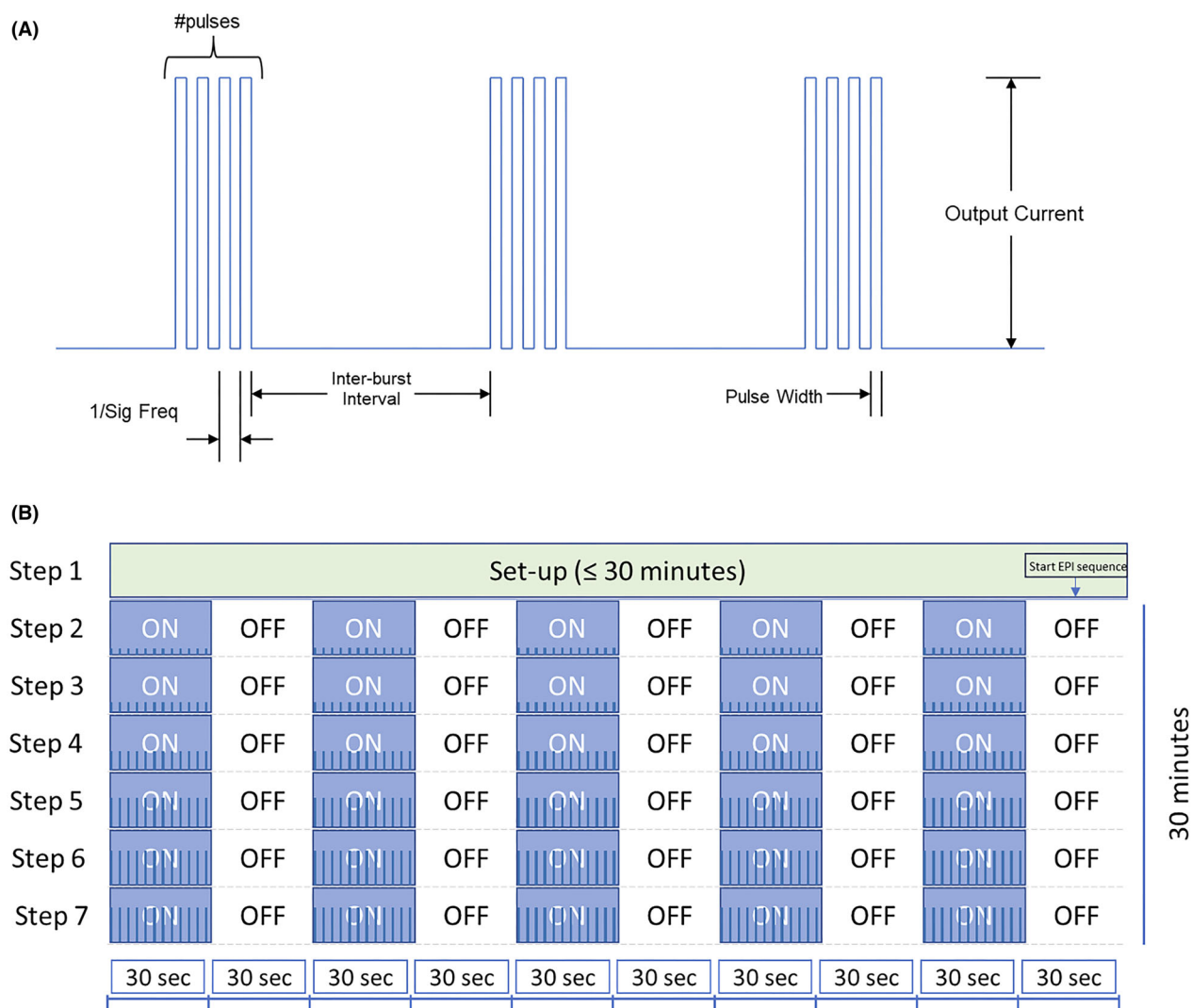


Figure 1. (A) Schematic of microburst stimulation train with specific parameter characteristics including number of pulses per burst, frequency of pulses, pulse width, interburst interval (time between bursts), and output current. (B) Schematic of typical scan during an MRI visit. For each of the three MRI scans, Step 1 (VNS is OFF) lasted up to 30 min to allow for participant placement in MRI scanner and acquisition of localizer and T1-weighted 3D anatomical scans. The start of the parameter sweep at Step 2 was manually synced to the start of the 30 min fMRI scan. Starting at Step 2, each fMRI scan was a blocked design where stimulation was provided for 30 sec (ON), followed by no stimulation for 30 sec (OFF). Each stimulation step was assessed for 5 min (i.e., 5 ON and 5 OFF blocks). The protocol allowed up to six stimulation steps (Steps 2–7) during the 30-min fMRI. Blue bars within the ON steps depict increasing intensity of stimulation parameters as typical for scan 2 (microburst optimization step).

onset seizures and to determine if the peak BOLD signal responses to standard VNS parameters are different from the peak responses elicited by an optimized microburst stimulation paradigm (i.e., assess for potential differences in the MOA). Further, for the first time, we wanted to conduct this neuroimaging investigation in stimulation-naïve epilepsy participants to determine if the pre-VNS treatment fMRI activation patterns (rather than longitudinal patterns) are associated with treatment response.^{2,16} Our hypotheses were that while both stimulation

parameters (standard vs. microburst) would involve thalamic responses, there would be differences in extra-thalamic VNS responses between the groups.

Material and Methods

Participants

Thirty-three adult patients with drug-resistant epilepsy were prospectively recruited (Table 1), and 29 were

Table 1. Clinical and epilepsy characteristics of focal- and generalized-onset seizure patients included in the study.

	Generalized-onset seizures (<i>N</i> = 10)	Focal-onset seizures (<i>N</i> = 19)	Total (<i>N</i> = 29) ¹
Age (years)			
Mean (SD)	25.5 (±9.7)	31.6 (±13.3)	29.5 (±12.4)
Sex (female/%)	6 (60%)	9 (47.4%)	15 (51.7%)
Race			
American Indian or Alaska Native	0	0	0
Asian	0	0	0
Black or African American	0	3 (15.8%)	3 (10.3%)
Native Hawaiian or Other Pacific Islander	0	0	0
White	10 (100%)	16 (84.2%)	26 (89.7%)
Other	0	0	0
Ethnicity			
Hispanic or Latino	0	2 (10.5%)	2 (6.9%)
Not Hispanic or Latino	10 (100%)	17 (89.5%)	27 (93.1%)
Primary seizure type ¹			
Focal impaired awareness seizures	0	10 (52.6%)	10 (34.5%)
Focal to bilateral seizures	0	8 (42.1%)	8 (27.6%)
Unknown onset seizures	0	1 (5.3%)	1 (3.4%)
Generalized seizures	10 (100%)	0	10 (34.5%)
Previous brain surgery	0	6 (31.6%)	6 (20.7%)
Time from epilepsy diagnosis to implant (years)			
<i>N</i>	7	12	19
Mean (SD)	7.9 (±5.9)	20.2 (±19.9)	15.7 (±17.1)
Number of ASMs the participant failed (SD)	6.6 (±4.8)	4.5 (±2.4)	5.2 (±3.5)
Range	2–17	2–10	2–17
Baseline number of ASMs	3.1 (±1.1)	2.8 (±0.9)	2.9 (±1.0)
Range	1–5	2–5	1–5
Seizure frequency (seizures/month) ²			
Baseline seizure frequency (SD)	20.1 (26.4)	24.0 (27.1)	22.9 (26.4)
6-month seizure frequency (SD)	3.4 (3.9)	13.6 (19.1)	10.8 (16.9)
12-month seizure frequency (SD)	3.2 (3.1)	8.8 (11.7)	7.2 (10.3)
Percent change in seizure frequency ²			
Baseline to 6-month (SD)	−59.3 (49.0)	−49.2 (33.9)	−52.0 (37.9)
Baseline to 12-month (SD)	−63.6 (48.3)	−67.2 (30.2)	−66.2 (35.1)
Percent change in seizure frequency ²			
Baseline to 6-month median (range)	−73 (−100 to +38)	−42 (−92 to +24)	−43 (−100 to +38)
Baseline to 12-month median (range)	−83 (−100 to +25)	−65 (−100 to −19)	−75 (−100 to +25)

¹Participating institutions and number of patients enrolled: University of Alabama at Birmingham (*n* = 3), Rush University Medical Center (*n* = 5), Northwestern University (*n* = 5), University of Colorado in Denver (*n* = 6), Mayo Clinic in Florida (*n* = 4), Weill Cornell Medical College (*n* = 1), Duke University (*n* = 5), University of Utah Health Science (*n* = 1), and Ghent University (*n* = 3). Data collected at Ghent University were not included in analyses due to restrictions imposed by the European Union Data Protection Laws. One participant from Duke University signed the informed consent but did not proceed to implantation and is not included in the analyses.

²Data provided for the 25 participants included in correlation analysis (*N* = 7 for generalized-onset seizures and *N* = 18 for focal-onset seizures)—see text for further explanation and calculation/exclusion of outliers. All participants showed improvement in seizures except for one with generalized-onset seizures and one with focal-onset seizures at 6 months, and the same one with generalized-onset seizures at 12 months.

available for analyses. One participant did not have thalamic activation and was excluded from MRI analyses. This limited the fMRI analyses to 28 participants who received initial (Visit 1) scans with standard and microburst stimulation parameters. Drug-resistant epilepsy status was established by review of medical records and confirmed by study epilepsy physician at each site. Participants had to be eligible for surgical implantation of a

VNS device and able and willing to undergo 3T MRI after implantation.² All participants provided written informed consent prior to participation, and all study procedures were approved by the Institutional Review Boards of each site. Demographic variables including type of seizure onset (e.g., focal vs. generalized) and baseline, 6- and 12-month seizure frequencies were collected for each participant (Table 1).

MRI scan procedures and VNS stimulation during fMRI

It is important to note that MRI scanning with active VNS is not recommended with commercial VNS devices. The manufacturer advises VNS to be deactivated prior to scanning, and that other pertinent restrictions of the device's MR-conditional labeling are followed. In this study, an investigational VNS device (Model 1000C) based on the foundation of the MR-conditional platform (Model 1000 "SenTiva") was approved under an Investigational Device Exemption to permit MRI data acquisition while the device was actively stimulating the vagus nerve. The changes associated with this device made it possible to assess multiple stimulation settings in the scanner (the "steps" described below). 3T MRI scanning parameters were tested and matched as closely as possible across sites prior to initiation of data collection. Using a transmit/receive head coil, minimum scan parameter requirements for each site were as follows: high resolution 3D T1-weighted anatomical scan with no larger than 1 mm thick contiguous slices and whole-brain coverage; T2*-weighted fMRI scan with TR 3000 ms and voxel size not larger than 4x4x4 mm³. However, all sites acquired T2*-weighted fMRI voxel resolution of 3x3x3 mm³ and 603 fMRI volumes including 3 "dummy" volumes that were discarded prior to preprocessing steps described below. Table 2 provides the scanning parameters for each site. For each participant, up to four postimplantation MRI visits were planned: at 2 weeks, 1, 3, and 6 months.

At each visit, 3 fMRI scans were conducted (Scan 1, 2, 3), with ~60 min breaks in between. Each scan was coordinated with 7 "steps" that were programmed into the VNS device (Fig. 1B). The protocol allowed for acquisition of the anatomical scan and up to 6 stimulation steps within the 1 h MRI scan. The current analysis presents only cross-sectional data from Visit 1 to investigate the possible differences in response to standard vs microburst parameters in VNS-naive epilepsy patients (MOA investigation).

Prior to each of the three fMRI scans, the participant's tolerance to increasing stimulation currents and the maximal-tolerated current (standard and microburst) were assessed to ensure stimulation during the fMRI would be well-tolerated. This was performed to ensure that any stimulation delivered during the fMRI was comfortable and would not contribute to significant movement during the imaging. Step 1 (Fig. 1B) duration for each of the three scans was set for up to 30 min of no stimulation to allow for participant placement in the MRI scanner. Participants were fitted with MR-compatible headphones to protect their hearing during the scan and to hear instructions from the study staff. Participants could be heard via a microphone and were also given an emergency bulb in case of distress/emergency during the scan. Step 1 was also the time during which the localizer and T1-weighted 3D anatomical scans were acquired. The start of the parameter sweep at Step 2 was manually synchronized to the start of the 30-min fMRI scan. Starting at Step 2, each fMRI scan was block-design with

Table 2. Description of the eight MRI scanners and the fMRI parameters included in analysis.

Site	3 Tesla Scanner		fMRI parameters				
	Manufacturer	Model	TR/TE	Flip angle	FOV	Voxel size	No. slices
University of Alabama at Birmingham	Siemens	Magnetom Prisma	3000 ms/ 25.0 ms	84	256 × 256 × 138	3 × 3 × 3 mm ³	46
Rush University Medical Center	Siemens	Magnetom Verio syngo	3000 ms/ 25.0 ms	84	256 × 256 × 132	3 × 3 × 3 mm ³	44
Northwestern University	Siemens	Magnetom Prisma fit	3000 ms/ 25.0 ms	84	256 × 256 × 138	3 × 3 × 3 mm ³	46
University of Colorado, Denver	Siemens	Magnetom Skyra	3000 ms/ 25.0 ms	84	256 × 256 × 138	3 × 3 × 3 mm ³	46
Mayo Clinic, Florida	Siemens	Magnetom Skyra	3000 ms/ 25.0 ms	84	256 × 256 × 138	3 × 3 × 3 mm ³	46
Weill Cornell Medical Center	GE	Signa Excite	3000 ms/ 25.0 ms	84	256 × 256 × 108	3 × 3 × 3 mm ³	36
Duke University	GE	Discovery MR750	3000 ms/ 25.0 ms	84	256 × 256 × 138	3 × 3 × 3 mm ³	46
University of Utah	Siemens	Magnetom Prisma fit	3000 ms/ 25.0 ms	84	256 × 256 × 138	3 × 3 × 3 mm ³	46

TR, repetition time; TE, echo time.

Table 3. Microburst programmable study stimulation parameters with the Model 3000C version 1.0 software.

Stimulation parameters	Programmable parameter settings (for each mode, i.e., Normal, Magnet, AutoStim)
Output current	0 to 2.00 mA incremented in 0.125 mA steps, 2.00 to 3.50 mA incremented in 0.25 mA steps
Signal frequency	100–350 pulses in 50 pulse per second increments.
Pulse width	100, 130, 150, 200, 250, 300, 350, 400, 450 and 500 μ sec
Pulses per set	4 or 7 (4 set as default)
Interburst interval	0.5, 1.5, or 2.5 sec
Signal ON time ^{1,2}	30 sec
Signal OFF time	0.5 min

¹Default On-time for Magnet Mode and AutoStim is 60 sec.

²AutoStim On-time is only available as 30 or 60 sec.

stimulation provided for 30 sec (ON), followed by no stimulation for 30 sec (OFF). Each stimulation step was assessed for 5 min (i.e., 5 ON blocks interleaved with 5 OFF blocks; Fig. 1B). The VNS stimulation parameters were set dependent on the Scan. For Scan 1, standard VNS stimulation parameters, for Scan 2, microburst VNS stimulation parameters, and for Scan 3, optimized microburst stimulation parameters were collected. Scans 1 and 2 focused on adjustments in current outputs while Scan 3 was designed to optimize microburst parameters (Table 3). In this study, peak BOLD signal changes in response to standard and optimized microburst parameters were compared (Scans 1 vs. Scan 3; see section 2.4 below). For Scan 1 (standard VNS), Steps 2–7 utilized standard VNS stimulation parameters that were optimized for current intensity of stimulation parameters based on participant's tolerability. For Scan 2, Steps 2–7 utilized microburst current intensity at a similar output to Scan 1. Microburst stimulation parameters optimized individually (Table 3) in Scan 2 (output current and signal frequency were adjusted while keeping other stimulation parameters constant, that is, pulse width at 250, pulses per set at 7, and interburst interval at 2.5) were tested in Scan 3 where the Steps 2–7 used each of the seven parameters optimized to output current stimulation level associated with peak thalamic response from Scan 2. Scan 3 parameters associated with peak thalamic response determined the participant's VNS settings until the follow-up visit.

MRI data preprocessing and analysis

fMRI data were analyzed and visualized using Analysis of Functional NeuroImages (AFNI).²⁰ Standard preprocessing algorithms²¹ were performed for each participant's fMRI dataset including removal of nonbrain voxels, co-

registration to anatomical MRI, slice-timing and motion correction, normalization to Talairach standard space (involved resampling anatomical MRI to $3 \times 3 \times 3$ mm³ voxel resolution to match resolution of fMRI images), calculating signal outliers (using *3dToutcount*), spatial smoothing to 5 mm full-width at half-maximum (FWHM) Gaussian filter, and calculation of percent signal change.

Single-subject general linear modeling of the fMRI BOLD response to each event type of ON, OFF, and the contrast of ON vs. OFF blocks (accounting for head motion and MRI signal drift) to determine VNS-related fMRI activation for each stimulation paradigm (i.e., Scan) setting (i.e., Step) was performed using the *3dDeconvolve* program in AFNI. Additionally, time points for each subject in which greater than 3% of voxels were defined as signal outliers (usually due to head motion) were not included in the general linear model. An anatomical thalamic mask from the Automated Anatomical Labeling (AAL) atlas was used to extract the mean t-value for each thalamic cluster meeting the minimum thresholds (5% alpha level; 2-voxel minimum); the signal peak was selected using the highest mean thalamic t-value. For group analysis, linear regression analyses were performed using the *3dttest++* program in AFNI. To investigate potential baseline differences in standard and microburst VNS stimulation intensity at the peak thalamic BOLD response, paired t-test was performed. Due to lack of significant differences between standard stimulation (current) intensity (mean = 0.42 mA; SD = 0.26) and microburst stimulation intensity (mean = 0.36 mA; SD = 0.21; $P = 0.16$), current intensity was not used as a covariate in linear regression analyses. To investigate potential baseline differences in fMRI activation between seizure types prior to manipulation of stimulation settings, we first compared participants with focal- and generalized-onset seizures while covarying for study site separately for Scan 1 (standard VNS settings). Absent differences facilitated combining groups in subsequent analyses, while covarying for study site, seizure type, and number of antiseizure medications (ASMs) for each participant. Input data for linear regression corresponded to the signal peak identified for each individual's Scan 1 and Scan 3. Resulting group activation maps illustrate average fMRI activation with standard and optimized microburst VNS, and the fMRI response differences between each.

Multiple-comparison correction was performed for fMRI analysis using a spatial autocorrelation function (ACF) in AFNI's *3dFWHx* program which estimates values for the smoothness of noise in the fMRI data and then fit them to a mixed model that combines the Gaussian-shaped ACF with a mono-exponential function. The mixed model was then used in AFNI's *3dClustSim*

program to generate noise random fields, estimate the probability of false-positive clusters (using 10,000 Monte Carlo simulations) and determine the threshold for the number of voxels that have to be in a cluster to achieve a corrected $P < 0.05$ when using a voxelwise threshold of $P < 0.01$ (t -value is at least 2.7991 per voxel). The cluster size determined in this process for these analyses is 46 voxels (or a minimum cluster volume of 1242 cubic mm) and is set for nearest neighbor of 2 which requires the edges of voxels to touch for inclusion in a cluster.

We conducted exploratory analyses to investigate relationship between baseline activation for standard versus microburst VNS or for each separately, and seizure outcome after 6 and 12 months of microburst VNS using SAS 9.4. One participant did not return for the 6-month follow-up and was excluded from these analyses. Outliers for baseline seizure frequency data were identified by calculating the first and third quartiles ($Q1 = 5.4$; $Q3 = 40.2$) and the interquartile range ($IQR = Q3 - Q1 = 34.8$); values greater than $Q3 + 1.5 * IQR$ (92.4) were classified as outliers. Seizure frequency for two participants with generalized-onset seizures was classified as outliers and not included in these analyses. For each brain region showing significant differences in fMRI activation between Scan 1 and Scan 3, and for the anatomical thalamus region of interest (ROI), signal was extracted and Spearman correlation analyses were performed with percent change in seizures from baseline to 6 and 12 months of microburst VNS (Table 1). Significant relationships with $P < 0.05$ and medium effect sizes of at least $|0.30|$ or greater are reported.

Results

Thalamic fMRI responses were obtained for Scans 1 and 3 in 28 participants. There were no significant differences

between participants with focal vs. generalized seizure onset in their standard VNS fMRI activation during Scan 1. Therefore, groups were combined in subsequent analyses.

Group activation maps indicated that standard VNS elicited primarily thalamic activation while optimized microburst VNS showed widespread activation in addition to thalamus (Fig. 2; Table 4). Thalamic activation showed overlap for standard and optimized microburst VNS with peaks observed in the left lateral posterior nucleus (standard) and in the right medial dorsal nucleus (optimized microburst) of the thalamus. Comparison of stimulation types revealed greater cerebellar, midbrain, and parietal fMRI activation in microburst VNS compared to standard VNS (Fig. 2C).

Exploratory analyses of the functional regions of interest (ROIs) from Figure 2C did not show any significant relationships or effect sizes of at least $|0.30|$, except that there was a medium effect size for the negative association between percent change in seizures after 12 months and baseline microburst VNS fMRI activation in the left midbrain extending to the fusiform regions ($\rho = -0.35$; $P = 0.087$) and in the left cerebellum ($\rho = -0.36$; $P = 0.076$). Exploratory analyses of baseline microburst VNS fMRI activation in the anatomical thalamus ROI showed a medium effect size for its negative association with percent change in seizures after 6 months ($\rho = -0.32$; $P = 0.12$), and then a significant negative correlation with percentage change in seizures after 12 months ($\rho = -0.40$; $P = 0.047$), but this did not survive correction for multiple comparisons.

Discussion

The goals of this study were to prospectively establish the typical brain response patterns to VNS using large cohort

Figure 2. Group data for vagus nerve stimulation (VNS) during fMRI ($n = 28$ subjects). The maximum tolerated stimulation output was determined out-of-scanner and used as the maximum setting for fMRI assessment. Group composite maps are based on peak thalamic activation for the (A) standard VNS parameters and (B) optimized novel microburst VNS parameters. Orange/yellow clusters illustrate VNS-related fMRI signal increases. Standard and microburst VNS elicit overlapping fMRI activation in the left lateral posterior nucleus and right medial dorsal nucleus of the thalamus as shown in the second row of panels in A and B. Coordinates for peak activation and extent of each cluster are provided in Table 4. Top rows show 4 sagittal slices at $x = -27$ and $x = -13$ in the left hemisphere and $x = +10$ and $x = 29$ in the right hemisphere; bottom rows focus on thalamic overlap and show two coronal slice at $y = -19$ and $y = -14$, and two axial slices at $z = +2$ and $z = +11$. (C) Significant differences in fMRI activations between the two stimulation types. Blue clusters indicate higher VNS-related activation for optimized microburst VNS compared to standard VNS. Row of 4 sagittal slices correspond with coordinates in A and B. A binary mask of clusters showing significant differences was created, and beta values within this mask were extracted from each subject's general linear modeling of the fMRI BOLD response of peak thalamic activation for each stimulation type. The numbers in the sagittal slices correspond to the cluster numbers in the graph. Beta values within the thalamus mask used to determine peak activation were also extracted and graphed. Group fMRI activation maps are overlaid onto a standard average brain in Talairach coordinate space. Activations are significant at corrected $\underline{P} < 0.05$ (voxelwise $\underline{P} < 0.01$ (t -value is at least 2.7991 per voxel), cluster extent threshold of 46 voxels (1242 mm³) in which sides of voxels must touch). Note that some clusters are large and within those clusters distinct anatomical brain regions coalesce. L = left, R = right, A = anterior, P = posterior, S = superior, I = inferior, IPL = inferior parietal lobule, AG = angular gyrus.

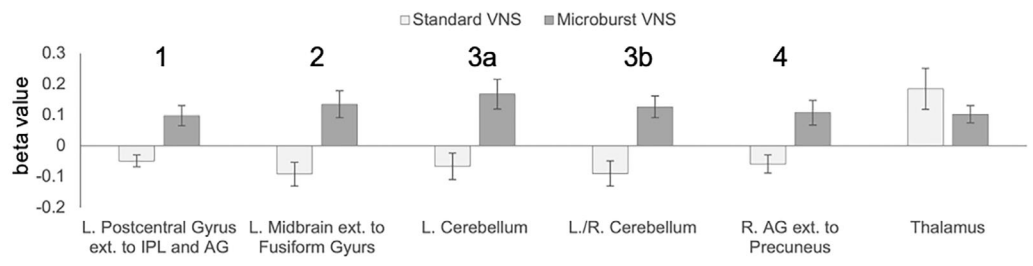
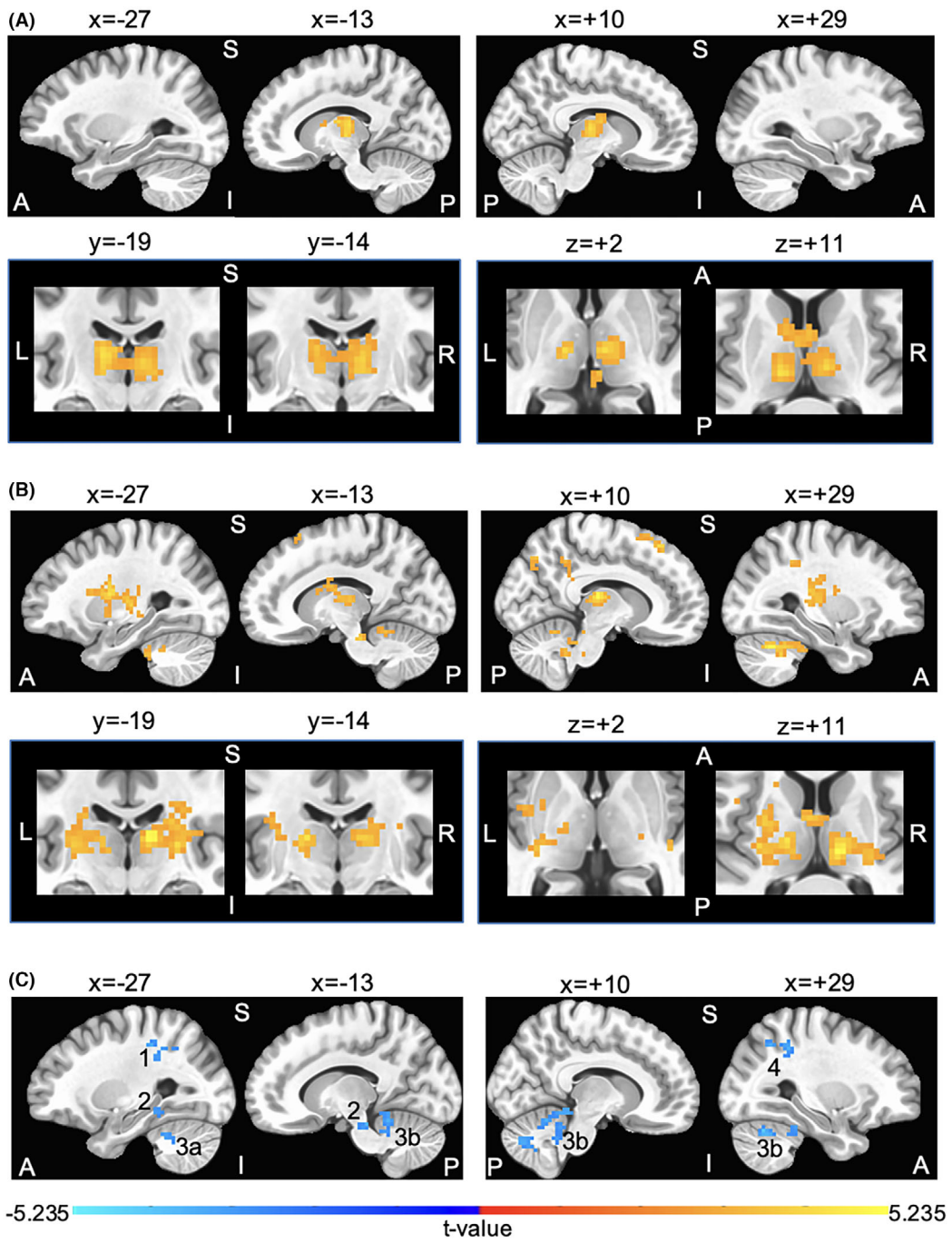


Table 4. Location and extent of brain regions in which patients exhibited (A) increased activation in response to stimulation using standard vagus nerve stimulation (VNS) parameters, (B) increased activation in response to stimulation using optimized microburst VNS parameters, and (C) differences in activation in response to stimulation using standard VNS compared to optimized novel microburst VNS parameters.

Brain regions	Peak coordinates (x, y, z)	Peak t-value	Cluster extent (mm ³)	
Standard VNS				
L. thalamus (lateral posterior nucleus)	-14, -19, 11	4.451	8262	
R. thalamus (medial dorsal nucleus)	7, -15, 2	4.404		
L. caudate	-10, 2, 11	3.436		
Microburst VNS				
L. insula	-35, -7, 20	4.663	11,907	
L. lentiform nucleus ext. to putamen	-25, -7, 14	4.391		
L. thalamus	-35, -7, 20	4.508		
L. caudate	-10, 5, 14	3.680		
L. IFG	-44, 2, 19	3.690		
L. SFG/BA6 ext. to mFG	-5, 16, 59	4.993		4050
R. SFG/BA6 (local peak)	5, 17, 60	4.425		
L. cerebellum	-23, -29, -37	3.681		1458
L./R. midline cerebellum	-5, -56, -22	4.352		
R. thalamus (medial dorsal nucleus)	11, -19, 11	5.138		7668
R. lentiform nucleus ext. to putamen	25, -18, 8	4.298		
R. insula	39, -22, 5	3.818	1647	
R. postcentral gyrus ext. to CG	27, -38, 39	4.098		
R. precuneus	13, -71, 44	4.189	1377	
R. cerebellum	28, -62, -31	5.132	5103	
R./L. midbrain	1, -26, -25	4.080	1323	
Microburst VNS > standard VNS				
L. postcentral gyrus ext. to IPL and AG	-26, -38, 47	-4.649	2025	
L. midbrain ext. to fusiform gyrus	-11, -29, -22	-4.464	1863	
L. cerebellum	-23, -50, -31	-3.979	1242	
L./R. midline cerebellum	-2, -62, -10	-4.663	8856	
R. cerebellum	28, -64, -27	-4.325	2241	
R. AG ext. to precuneus	27, -58, 45	-3.875		

Note that some clusters are large and distinct anatomical brain regions coalesce. L, left hemisphere; R, right hemisphere; ext., extending; IFG, inferior frontal gyrus; SFG, superior frontal gyrus; BA, Brodmann's Area; mFG, medial frontal gyrus; CG, cingulate gyrus; IPL, inferior parietal lobule; SPL, superior parietal lobule; AG, angular gyrus.

of patients with focal- and generalized-onset seizures, to determine whether the BOLD signal responses to standard VNS are different from those elicited by optimized microburst stimulation (i.e., assess for potential differences in the MOA), and to conduct a proof-of-concept multicenter study with BOLD signal responses as a guide for VNS stimulation parameters adjustments. We also wanted, for the first time, to conduct this neuroimaging investigation in stimulation-naïve epilepsy participants to determine if the pretreatment fMRI activation patterns are associated with treatment response in a longitudinal cohort (complete results are included in a separate report under review). Our hypotheses were that while brain BOLD signal responses to standard and microburst stimulation parameters would include thalami, there would be differences in extra-thalamic responses to VNS between the groups.

We did not identify any differences in brain activation for the standard stimulation approach between

participants with focal- and generalized-onset seizures. This allowed for the neuroimaging data to be combined for further analyses to include the highest to-date number of VNS-naïve participants in an fMRI study increasing our confidence in the observed results. Both groups exhibited robust BOLD signal changes in thalami permitting us to use these responses for microburst stimulation parameter optimization in Scan 3. When compared between groups, the thalamic BOLD signal intensity and extent were not significantly different between standard and optimized microburst stimulation parameter groups. However, the peaks of thalamic responses were somewhat differently localized between standard vs. microburst stimulation parameters (Table 3). Finally, optimized microburst parameters induced additional parietal (postcentral gyrus/inferior parietal lobule and angular gyrus/precuneus) and midline posterior fossa BOLD signal increases (midbrain, cerebellum). All these activations were expected based on previous studies that showed

similar activation patterns with various areas involved in VNS stimulation responses between studies.^{15–19,22}

Both stimulation paradigms modulate thalamic blood flow in a similar manner. Hence, it is likely that both approaches to VNS stimulation may result in similar thalamic modulatory effects. While the location of the thalamic peaks was different between stimulation parameters (Table 4), we cannot state with confidence that the differences are genuine. This is mostly because of the imaging parameters included large fMRI voxel size that was used in this study to facilitate collecting data between sites and accomplish the proof-of-concept goal of being able to conduct a multi-site fMRI VNS study. However, if the differences between standard and optimized microburst stimulation paradigms in the location of BOLD peaks are confirmed in future studies that use single scanner type and scanning parameters optimized for visualization of small thalamic structures, then we may be able to determine whether the differences in thalamic responses are predictive of long-term seizure and/or adverse events outcomes.¹⁶ We also need to recognize that the observed differences in thalamic (and other BOLD signal responses) may be related to the fact that microburst stimulation parameters were optimized (Scan 3) while standard stimulation parameter optimization was limited to current intensity; other stimulation parameters were not adjusted (e.g., pulse width, burst treatment duration or interburst interval). In previous work, optimization of one of the standard VNS stimulation parameters (pulse width) resulted in different BOLD signal responses.¹⁷ Further, BOLD signal responses can vary with multiple factors such as stimulus type and intensity, duration, age of the participants, and location of the brain region.^{23–25} Thus, it is also possible that with optimization testing the differences between standard and microburst stimulation results could become less or more pronounced. In this study, microburst optimization included multiple adjustment steps and two scans (Scan 2 and 3) and only data from the latter (Scan 3) were used for the comparisons; standard stimulation parameter scans were always collected first. While this was “by design,” this sequential approach to collecting imaging data precludes assessing whether any of the results related to microburst stimulation are truly related to the micro-stimulation parameters or whether they are the results of the sequence of data collection (i.e., standard first and microburst second) which may have already primed the network for modulatory changes. Further, iTBS is known to include residual network changes lasting for at least 60 min hence Scan 2 could have resulted in residual effects observed in Scan 3⁶ but this analysis is beyond the scope of the current study.

We also observed BOLD signal increases in bilateral parietal regions (angular gyrus/precuneus and postcentral

gyrus/inferior parietal lobule)—these patterns were relatively scattered and somewhat shifted between sides (Fig. 2). These changes were only observed in the optimized microburst VNS parameters, and the question is whether this pattern of activation provides an additional advantage. In at least one study, a visually similar widespread pattern of somatosensory evoked potential responses tested with magnetoencephalography (MEG) was observed in standard VNS-responders compared to nonresponders with additional differences between the groups noted in functional connectivity between the limbic and somatosensory cortices.²⁶ These authors specifically postulated a relationship between a more widespread modulation of cortical structures pre-VNS implantation and better VNS response. Thus, in agreement with that study, the response to microburst VNS observed in our study could potentially confer a treatment advantage. However, while some of the brain regions included in this response to microburst VNS are also involved in functions such as recollection memory and integration of spatial information,^{27,28} it is not clear whether these or other functions were affected here as this was not specifically studied. Therefore, the question of the advantages of microburst VNS over standard stimulation protocol for seizure control or cognitive function improvement remains, especially in view of the already observed positive effects of VNS on cognition²⁹ and the previously noted positive effect of microburst-type stimulation on LTP.⁸

Additional microburst-related fMRI activations included midbrain and cerebellum. While these regions are not typically considered as areas involved in seizure generation and maintenance, the literature may argue otherwise because of the extensive monosynaptic connections between the caudal and the rostral brain.³⁰ In fact, Heath implanted patients with severe mental illness (some with comorbid epilepsy) with cerebellar stimulator contacts located around rostral vermis³¹ to show 10/11 participants to have significant enough improvement in their symptoms to be released from the mental health hospital and functioning “without medical or other treatment.” This study also performed stimulation of or around the cerebellar vermis in patients with seizures and was able to document seizure spread interruption.³¹ These posterior fossa BOLD signal changes are also in agreement with the previous animal literature that showed VNS-induced cellular and metabolic changes in those regions.¹¹ Thus, it is not surprising that recent literature calls for reconsideration of the use of therapies that affect or modulate cerebellar architecture and connections.³² The involvement of cerebellum in our stimulation response certainly suggests that this notion may be able to be tested in this trial in longitudinal data.

Our correlational analyses of cross-sectional BOLD signal differences between stimulation groups revealed modest relationships with seizure response, with the largest effect size being the relationship between thalamic activation with microburst and seizure response at 12 months ($\rho = -0.40$; $P = 0.047$). While the paucity of significant relationships may be surprising in view of the postcentral and cerebellar discussion and in view of the PET data that showed a relationship between thalamic changes and seizure response,¹⁶ this relative discrepancy can be explained. First, the trends toward significance may become significant with improvements in scanning parameters, larger number of participants, or more homogeneous group of participants. Second, relationships between BOLD signal and seizure responses may be modulated by time such that BOLD relationship with multiple scanning sessions may be more revealing than a single cross-sectional pre-VNS time point; clinical responses to VNS are known to improve over time.² Finally, the only modest correlation between thalamic microburst and seizure outcomes may also be surprising. However, the original thalamic study was performed on longitudinal PET data while the results discussed here are based on pre-VNS cross-sectional measurements of BOLD signal changes. The longitudinal or connectivity analyses are outside the scope of this manuscript and will be presented and discussed separately.

There are several strengths of this study. This is a first study that utilized fMRI in patients with VNS to initiate and guide their treatment²; the study proved the concept of using fMRI for this purpose and also confirmed relative safety of using VNS with fMRI scanning. When completed and data are analyzed, this study will determine if the results of initial fMRI (standard vs. optimized microburst) correlate with seizure outcomes. If positive, these results may pave the way for designing neurostimulation and neuromodulation studies using fMRI not only as a neuro-navigation tool for stimulation site localization, but also as a tool that provides short-latency biomarker(s) for treatment response.⁷ However, this study also has limitations with the most important ones being the selection of the neuroimaging parameters and collection of imaging data on multiple scanners (Table 2). The imaging parameters were selected not necessarily for the optimization of structure and function visualization but rather for simplicity and ease of multi-site implementation; specific sites were not selected based on scanner uniformity but on their interest, ability to meet minimal study imaging parameters, and ability to recruit participants. Future studies may select sites with more advanced scanners and coils to allow fine tuning of the scanning parameters. The use of multiple scanners (Table 2) is also another disadvantage, and while we have accounted for this in our

analyses, we cannot state with certainty that some of our results are not related to this. Another weakness, as stated above, is the forced sequence of scans. While this was by design, we cannot exclude the possibility that lack of randomization resulted in priming effects impacting the results. However, maintaining at least 60 minutes between scans should have minimized these effects if present. Also, one participant did not exhibit thalamic BOLD signal response to microburst stimulation and had to be excluded from the analyses. We can only speculate the reasons for this lack of thalamic BOLD signal response (e.g., stimulation parameters not sufficiently high to elicit response) as the study was not designed to specifically test for this. We were unable to control the analyses for the type of medications used by the patient for controlling seizures and other comorbid conditions. It is well recognized that some of these medications may affect BOLD signals.^{33–35} It should be noted that while focal-onset seizures group had six patients with prior brain surgery, fMRI activation did not significantly differ from that of the generalized-onset seizures group in which none had prior brain surgery suggesting a negligible impact of previous brain surgery on the results. Furthermore, the within-subject design in comparing fMRI activation between standard versus microburst VNS minimized the potential impact of previous brain surgery. Finally, we did not optimize the standard VNS stimulation parameters as this was not a goal of this study. However, we cannot exclude the possibility that further optimization of the standard stimulation parameters could affect BOLD signal changes. Such adjustments are conducted daily by epilepsy providers in patients with already implanted VNS devices.

Conclusions

This study provides further human *in vivo* support for thalamic involvement in the MOA of VNS. It also documents the differences in the extent of brain involvement between standard and microburst stimulation paradigms. While this study did not specifically investigate whether involvement of midbrain or cerebellar vermis in microburst stimulation response is advantageous, previous data show involvement of these structures in response to seizures and indicate a potential target for treatment interventions.

Acknowledgements

This study was supported by LivaNova Inc. Dr. Szaflarski and Dr. Allendorfer received continuous consulting support for study development, implementation, and for data analysis pipeline development and implementation. Final

data analyses and reporting were supported by a separate grant from LivaNova Inc. to JPS. Drs. Begnaud, Ranuzzi, Shamshiri, and Verner are employees of LivaNova Inc. The Microburst Study Group was comprised of industry and academic partners including Rebecca O'Dwyer (Rush University), Michael Macken (Northwestern University), Blake Newman (University of Utah), Cornelia Drees (University of Colorado), Danielle McDermott (University of Colorado), Lesley Kaye (University of Colorado), Mesha Gay Brown (University of Colorado), Muhammad Zafar (Duke University), William Tatum (Mayo Clinic), Selim Benbadis (University of South Florida), Pegah Afra (Cornell-Weill), Zeenat Jaisani (University of Alabama at Birmingham), and Kristl Vonck (UZ Gent). LivaNova contributors included Amy Keith, Gaia Giannicola and the Clinical Affairs and Clinical Engineering staff. ^aMicroburst study group includes: Danielle McDermott, MD, University of Colorado School of Medicine; Mesha Gay Brown, MD, University of Colorado School of Medicine; Michael Macken, MD, Northwestern University Feinberg School of Medicine; Irena Bellinski, Northwestern University Feinberg School of Medicine; Elizabeth Cunningham, Northwestern University Feinberg School of Medicine; Rebecca O'Dwyer, MD, Rush University Medical Center; Fiona Lynn, MSN, APRN, Rush University Medical Center; William O. Tatum, DO, Mayo Clinic Florida; Selim R. Benbadis, MD, University of South Florida Morsani School of Medicine; Zeenat Jaisani, MD, University of Alabama at Birmingham; Muhammad Zafar, MD, Duke University Hospital; Blake Newman, MD, University of Utah School of Medicine; Seyhmus Aydemir, MD, Weill-Cornell Medical Center; Kristl Vonck, MD, PhD, Ghent University Hospital; Ann Mertens, MD, PhD, Ghent University Hospital; Cornelia Drees, MD, Mayo Clinic Arizona; Pegah Afra, MD, University of Massachusetts Chan Medical School; Leslie Kaye, MD, University of Colorado School of Medicine; [Charles Gordon, Amy Keith, Steffen Fetzer, PhD, Mei Jiang, Gaia Giannicola, PhD, Wim Van Grunderbeek], LivaNova PLC (or a subsidiary).

Author Contributions

All authors made substantial, direct, and intellectual contributions to this work. Conceptualization and study development: JPS and JBA. Data acquisition: JB and GG. Data processing and visualization: JBA. Writing of the first draft: JPS. Writing—editing and review: all authors.

Data Availability Statement

Due to current privacy concerns, data sharing is not possible.

References

1. Bolden L, Pati S, Szaflarski J. Neurostimulation, neuromodulation, and the treatment of epilepsies. *J Epileptol.* 2015;23:45-59.
2. Verner R, Szaflarski JP, Allendorfer JB, Vonck K, Giannicola G, Microburst Study Group. Modulation of the thalamus by microburst vagus nerve stimulation: a feasibility study protocol. *Front Neurol.* 2023;14:1169161.
3. Touma L, Dansereau B, Chan AY, et al. Neurostimulation in people with drug-resistant epilepsy: systematic review and meta-analysis from the ILAE Surgical Therapies Commission. *Epilepsia.* 2022;63:1314-1329.
4. Denison T, Morrell MJ. Neuromodulation in 2035: the neurology future forecasting series. *Neurology.* 2022;98:65-72.
5. Ziemann U, Hallett M, Cohen LG. Mechanisms of deafferentation-induced plasticity in human motor cortex. *J Neurosci.* 1998;18:7000-7007.
6. Huang YZ, Edwards MJ, Rounis E, Bhatia KP, Rothwell JC. Theta burst stimulation of the human motor cortex. *Neuron.* 2005;45:201-206.
7. Shah PP, Szaflarski JP, Allendorfer J, Hamilton RH. Induction of neuroplasticity and recovery in post-stroke aphasia by non-invasive brain stimulation. *Front Hum Neurosci.* 2013;7:888.
8. Gamboa OL, Antal A, Moliadze V, Paulus W. Simply longer is not better: reversal of theta burst after-effect with prolonged stimulation. *Exp Brain Res.* 2010;204:181-187.
9. Ito S, Craig AD. Vagal-evoked activity in the parafascicular nucleus of the primate thalamus. *J Neurophysiol.* 2005;94:2976-2982.
10. Ito S, Craig AD. Striatal projections of the vagal-responsive region of the thalamic parafascicular nucleus in macaque monkeys. *J Comp Neurol.* 2008;506:301-327.
11. Naritoku DK, Terry WJ, Helfert RH. Regional induction of fos immunoreactivity in the brain by anticonvulsant stimulation of the vagus nerve. *Epilepsy Res.* 1995;22:53-62.
12. Farrand A, Jacquemet V, Verner R, Owens M, Beaumont E. Vagus nerve stimulation parameters evoke differential neuronal responses in the locus coeruleus. *Physiol Rep.* 2023;11:e15633.
13. Cooper CM, Farrand AQ, Andresen MC, Beaumont E. Vagus nerve stimulation activates nucleus of solitary tract neurons via supramedullary pathways. *J Physiol.* 2021;599:5261-5279.
14. Alexander GM, McNamara JO. Vagus nerve stimulation elevates seizure threshold in the kindling model. *Epilepsia.* 2012;53:2043-2052.
15. Henry TR, Bakay RA, Votaw JR, et al. Brain blood flow alterations induced by therapeutic vagus nerve stimulation in partial epilepsy: I. Acute effects at high and low levels of stimulation. *Epilepsia.* 1998;39:983-990.

16. Henry TR, Votaw JR, Pennell PB, et al. Acute blood flow changes and efficacy of vagus nerve stimulation in partial epilepsy. *Neurology*. 1999;52:1166-1173.
17. Mu Q, Bohning DE, Nahas Z, et al. Acute vagus nerve stimulation using different pulse widths produces varying brain effects. *Biol Psychiatry*. 2004;55:816-825.
18. Liu WC, Mosier K, Kalnin AJ, Marks D. BOLD fMRI activation induced by vagus nerve stimulation in seizure patients. *J Neurol Neurosurg Psychiatry*. 2003;74:811-813.
19. Narayanan JT, Watts R, Haddad N, Labar DR, Li PM, Filippi CG. Cerebral activation during vagus nerve stimulation: a functional MR study. *Epilepsia*. 2002;43:1509-1514.
20. Cox RW. AFNI: software for analysis and visualization of functional magnetic resonance neuroimages. *Comput Biomed Res*. 1996;29:162-173.
21. Goodman AM, Diggs MD, Balachandran N, et al. Repeatability of neural and autonomic responses to acute psychosocial stress. *Front Neurosci*. 2020;14:585509.
22. Sucholeiki R, Alsaadi TM, Morris GL 3rd, Ulmer JL, Biswal B, Mueller WM. fMRI in patients implanted with a vagal nerve stimulator. *Seizure*. 2002;11:157-162.
23. Boynton GM. Spikes, BOLD, attention, and awareness: a comparison of electrophysiological and fMRI signals in V1. *J Vis*. 2011;11:12.
24. de Munck JC, Goncalves SI, Huijboom L, et al. The hemodynamic response of the alpha rhythm: an EEG/fMRI study. *NeuroImage*. 2007;35:1142-1151.
25. Grady CL, Garrett DD. Understanding variability in the BOLD signal and why it matters for aging. *Brain Imaging Behav*. 2014;8:274-283.
26. Mithani K, Wong SM, Mikhail M, et al. Somatosensory evoked fields predict response to vagus nerve stimulation. *Neuroimage Clin*. 2020;26:102205.
27. Cavanna AE, Trimble MR. The precuneus: a review of its functional anatomy and behavioural correlates. *Brain*. 2006;129:564-583.
28. Donnelly KM, Allendorfer JB, Szaflarski JP. Right hemispheric participation in semantic decision improves performance. *Brain Res*. 2011;1419:105-116.
29. Desbeaumes Jodoin V, Richer F, Miron JP, Fournier-Gosselin MP, Lesperance P. Long-term sustained cognitive benefits of Vagus nerve stimulation in refractory depression. *J ECT*. 2018;34:283-290.
30. Heath RG. Brain function in epilepsy: midbrain, medullary, and cerebellar interaction with the rostral forebrain. *J Neurol Neurosurg Psychiatry*. 1976;39:1037-1051.
31. Heath RG. Modulation of emotion with a brain pacemaker. Treatment for intractable psychiatric illness. *J Nerv Ment Dis*. 1977;165:300-317.
32. Streng ML, Krook-Magnuson E. The cerebellum and epilepsy. *Epilepsy Behav*. 2021;121:106909.
33. Beltramini GC, Cendes F, Yasuda CL. The effects of antiepileptic drugs on cognitive functional magnetic resonance imaging. *Quant Imaging Med Surg*. 2015;5:238-246.
34. Nenert R, Allendorfer JB, Bebin EM, et al. Cannabidiol normalizes resting-state functional connectivity in treatment-resistant epilepsy. *Epilepsy Behav*. 2020;112:107297.
35. Szaflarski JP, Allendorfer JB. Topiramate and its effect on fMRI of language in patients with right or left temporal lobe epilepsy. *Epilepsy Behav*. 2012;24:74-80.